APPLICATION OF EULER DECONVOLUTION TECHNIQUE IN DETERMINING DEPTHS TO MAGNETIC STRUCTURES IN MAGADI AREA, SOUTHERN KENYA RIFT

J. G. Githiri[1], J. P. Patel[2], J. O. Barongo[3] and P. K. Karanja[4]
[1,4]Department of Physics, Jomo-Kenyatta University of Agriculture, Science and Technology, Nairobi
[2,3]University of Nairobi, Kenya
E-mail: githiri@fsc.jkuat.ac.ke

Abstract

Magadi area is located in the southern part of the Kenyan rift, an active continental rift that is part of the East African Rift system. Thermal manifestations in the form of hot springs in the northern and southern shores of Lake Magadi and high heat flows suggest geothermal potential in the area. A ground magnetic survey was carried out in the study area with the aim of locating depths to bodies with sufficient magnetic susceptibility that may represent magmatic intrusions. The magnetic data was corrected, a total intensity magnetic contour map produced and profiles drawn across identified anomalous regions. Magnetic survey data in profile form over anomalous regions was interpreted rapidly for source positions and depths by Euler deconvolution technique. Geologic constraint was imposed by use of a structural index 1.0 that best describes prismatic bodies such as intrusive dykes. The magnetic bodies were imaged at depths ranging from 0 km to about 11 km along the profiles. The imaged depths along the profiles display discontinuities in magnetic markers due to presence of numerous faults in the area. The detected magnetic bodies may be cooling dykes that heat the underground water responsible for the numerous hot springs surrounding Lake Magadi. Such a dyke is suspected to originate from a magma chamber conducting heat to the underground water. A model whereby the faults in the region provide escape of water as hot springs is proposed.

Key words: Magnetic, magadi area, geothermal, deconvolution

1.0   Introduction

Magadi area which is the study area is bounded by latitudes 1° 40´ S and 2° 10´ S, longitudes 36° 00´ E and 36° 30´E as illustrated in Figure 1. The area is located in the southern part of the Gregory Rift, an active continental rift that is part of the East African rift system. The Gregory Rift is of the continental type Gregory (1921). It extends from the Magadi-Natron basin in the south to Baringo and Suguta grabens in the north. The southern part of the Kenya rift is a region of geodynamic activity expressed by recent volcanism. Lake Magadi is located in a broad flat depression that occurs at the lowest point in the southern Kenya Rift Valley. Geothermal fields are present in Magadi characterised by fissure eruptions, which are trachytic in composition. Hot springs are distributed along the shores of Lake Magadi issuing from the base of fault scarps. The study was carried out with a view to understanding the subsurface structure of the greater Magadi area by investigating possibility of presence of magnetic bodies that may be heat sources.

Geologically, Magadi area is classified into three formations by Baker (1958 and 1963) namely precambrian metamorphic rocks, plio-pleistocene volcanics, the holocene to recent lake and fluvial sediments. The basement rocks outcrop in the region west of the Nguruman escarpment. These rocks consist mainly of regular banded schists, gneisses and muscovite-rich quartzites. The basement rocks are overlain by the Kirikiti platform, which is down faulted to the rift floor at the Nguruman Escarpment. Baker (1958) found that the olivine basalt layers of the Kirikiti platform are interbedded with conglomerates; gravels and sands deposited between different eruption episodes. The area has three central volcanoes, namely, Olorgesailie, Lenderut and Shompole. Olorgesailie is the highest, its lava composition consisting of olivine basalts, alkali trachyte and nephelinite. Further south, Lenderut Volcano dated 2.5 million years (Ma) has basalt and andesite lavas, while Shompole dated 2.0 Ma consists of carbonatite and nephelinite rocks.
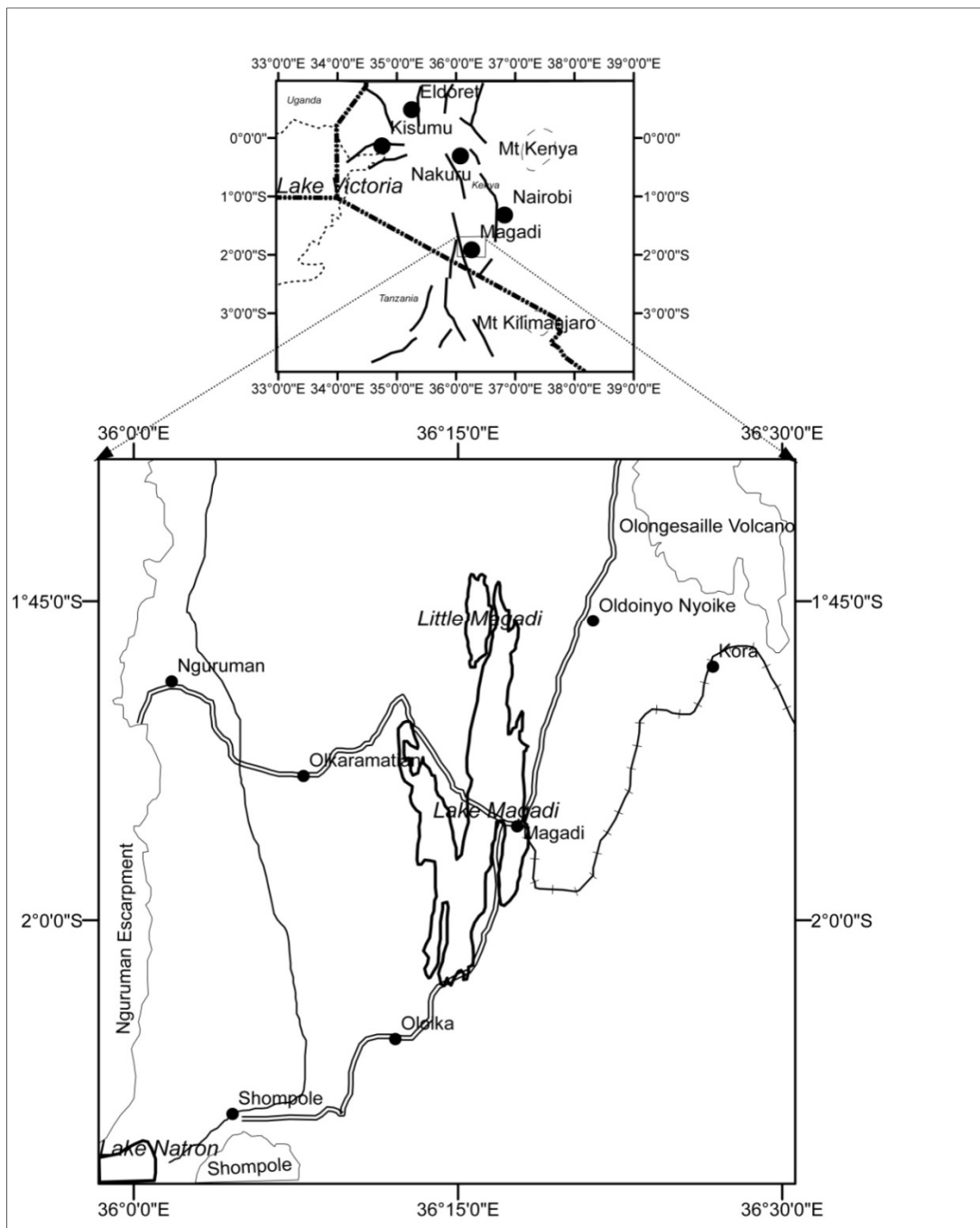
Figure 1: Location map of study area.

 The most extensive volcanic activity in the area occurred between 1.4 and 0.7 Ma. During this activity the Magadi Plateau trachytes series were formed. The location of study area is as displayed in Figure 2.
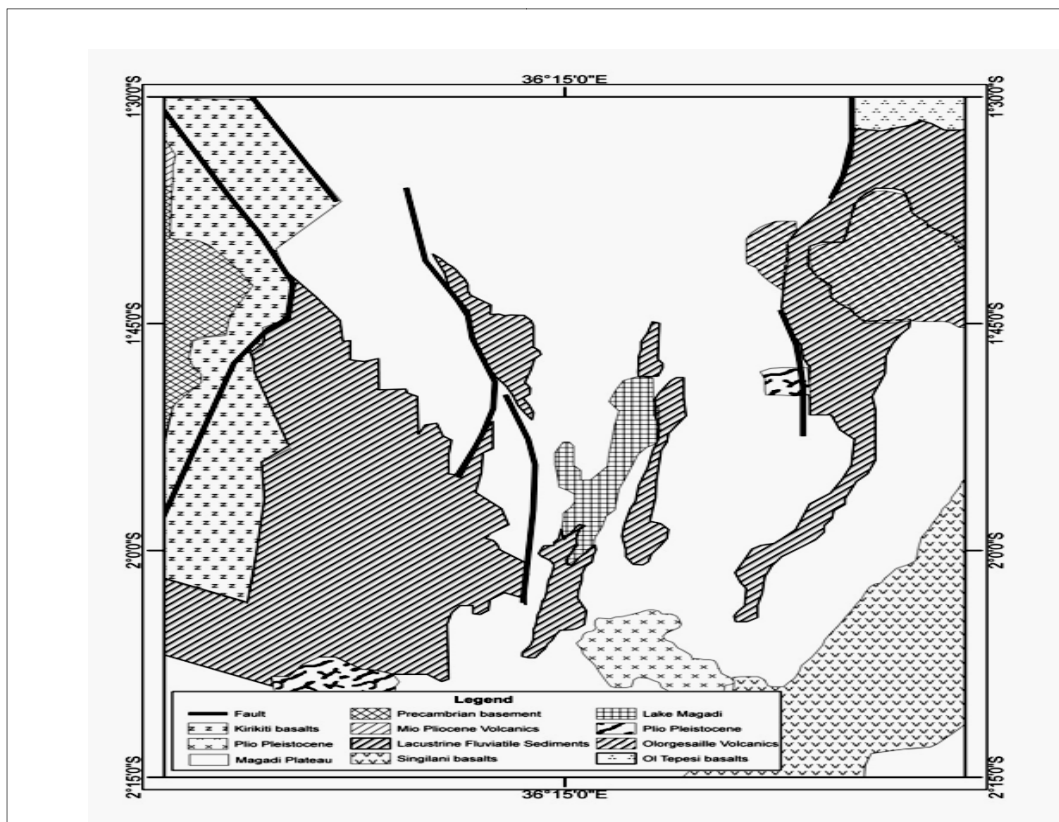

Figure 2: Geological map of Magadi (simplified from Baker, 1958, 1963).

2.0   Methodology

Establishing and positioning of magnetic stations including base stations was done using a global positioning system (GPS). A total of 58 magnetic stations were established. The total magnetic field intensity was measured at each station using a proton precession magnetometer model G-856 with an accuracy of 0.1 nT. A single proton precession magnetometer was used in the survey and therefore a base station was chosen at the beginning of a day's work and reoccupied after about every two hours and diurnal variations carried out. Normal geomagnetic corrections were neglected in this study as the survey area was considered small relative to geological features of interest. The residual total magnetic field intensity map (Figure 3) was prepared with contour intervals of 25 nT. Solid contours were used to represent magnetic highs, while hachured contours represent magnetic lows. Profiles were selected from the total intensity magnetic map passing through the discerned anomalies.

Euler Deconvolution Technique

Euler deconvolution is a technique, which uses potential field derivatives to image subsurface depth of a magnetic or gravity source (Hsu, 2002). Mushayandebvu *et al.* (2001) described 2D space Euler's deconvolution equation as

$$\left(X - X_0\right)\frac{\partial T}{\partial X} + \left(Z - Z_0\right)\frac{\partial T}{\partial Z} = -N\Delta T \, ,\dots\dots\dots\dots\dots\dots\dots\dots\dots\dots\dots\dots\dots\dots(1)$$

where (X_0, Z_0) is the coordinate position of the top of the body, Z is the depth measured as positive down, X the horizontal distance, ΔT the value of the residual field, and N the structural index. The structural index is a measure of the rate of change or fall off rate with distance of a field and therefore it is a function of the geometry of the causative bodies. Thus, the magnetic field of a point dipole falls off as the inverse cube, giving an index of three, while a vertical line source gives an inverse square field fall off and an index of two. Extended bodies will form assemblages of dipoles and will therefore have indices ranging from zero to three.

If ΔT_i is the residual field at the ith point in a magnetic or gravity survey, with the point of measurement at (X, Z) and the coordinate position of the top of the body (X_0, Z_0), then equation 1 can be written as,

$$\begin{bmatrix} \dfrac{\partial}{\partial x}\Delta T_i & \dfrac{\partial}{\partial z}\Delta T_i \end{bmatrix}\begin{bmatrix} X - X_0 \\ Z - Z_0 \end{bmatrix} = N\Delta T_i \, ,\dots\dots\dots\dots\dots\dots\dots\dots\dots\dots\dots\dots\dots\dots(2)$$

By calculating the horizontal and vertical gradients of the field, equation 2 has only three unknowns X_0, Z_0 and N, where the first two describe the location of the body. Many simultaneous equations can be obtained for various measurement locations which can give rise to one matrix equation.

$$\begin{bmatrix} \dfrac{\partial}{\partial x}\Delta T_1 & \dfrac{\partial}{\partial z}\Delta T_1 \\ \dfrac{\partial}{\partial x}\Delta T_2 & \dfrac{\partial}{\partial z}\Delta T_2 \\ - & - \\ \end{bmatrix}\begin{bmatrix} X - X_0 \\ Z - Z_0 \end{bmatrix} = N\begin{bmatrix} \Delta T_1 \\ \Delta T_2 \\ - \end{bmatrix}\dots\dots\dots\dots\dots\dots\dots\dots\dots\dots\dots\dots\dots(3)$$

The least squares method can be used to obtain the unknowns X_0 and Z_0 if the structural index N is known. EULER 1.0, a two dimensional software by Cooper, (personal communication) was used for imaging the magnetic sources, where the 2D space defines depth (Z) positive down and horizontal distance (X).
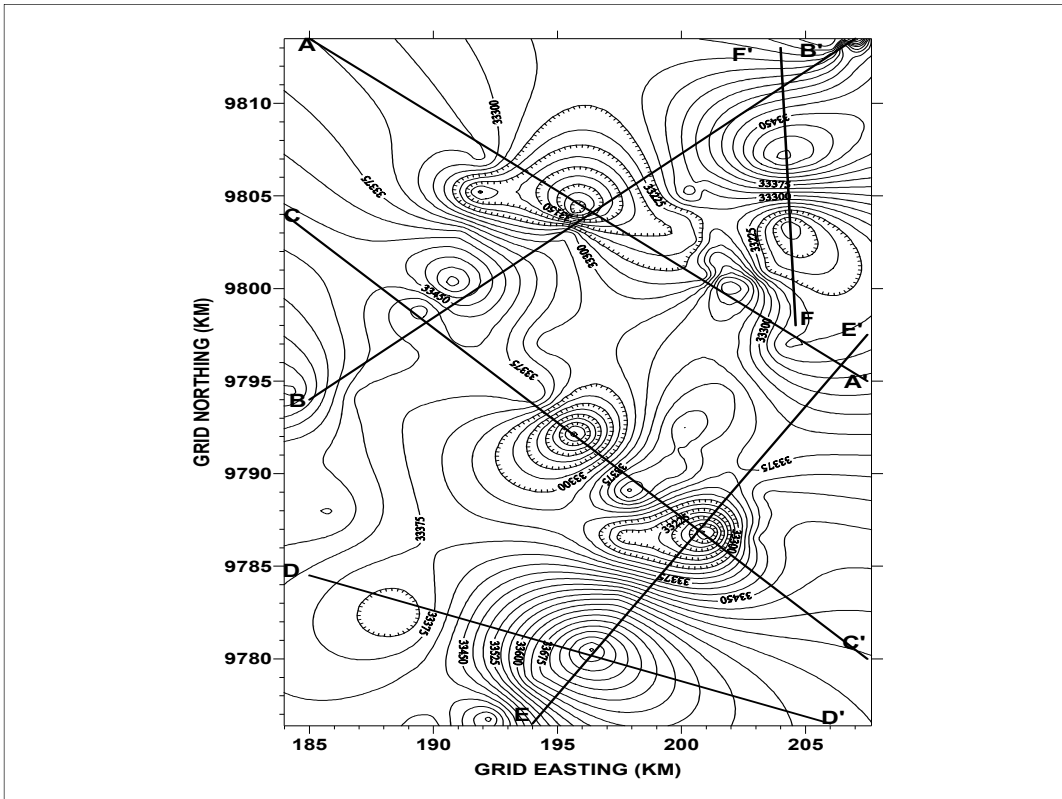
Figure 3: Magnetic intensity contour map

The input data to the software was profile magnetic data. For the magnetic Euler solutions other than profile data, other input information included magnetic inclination, declination and the background normal total magnetic field. Magnetic declination of value 1º 56˚ was used for the study area as from topographic map sheet 160/4 printed by survey of Kenya. By qualitative interpretation of the magnetic contour map's quiet areas, a normal total field was approximated as 33300 nT. The magnetic inclination of -25.27º of the area was also imputed. The source distribution is assumed to be two-dimensional such that the first derivatives of T that is $\dfrac{\partial T}{\partial X}$ and $\dfrac{\partial T}{\partial Z}$ at all the above locations are calculated by the software. When magnetic data in a profile is run in EULER 1.0 software, the profile is divided into windows of set of data points ranging from 7 to 19. A source location (X_0, Z_0) is calculated for each set of points using equation 3 and least-squares methods. Source locations were plotted in cross-section, which clustered around magnetised sources. Table 1 displays structural indices for different possible geological structures.

Table 1: Structural indices for different geological structures (after Reid etal. 1990)

Structural Index	Geological Structure
0	Contact

0.5	Thick Step
1	Sill / Dike
2	Vertical Pipe
3	Sphere

2.2   Boundary Analysis By Horizontal Gradients

The steepest horizontal gradient of a pseudo gravity anomaly caused by buried cylindrical body tends to occur at the edges of the body. The steepest gradient is located over the edge of the body if the edge is vertical and far removed from all other edges or sources. This is applied to magnetic measurements by first transforming them into pseudo gravity anomalies, in which the steepest horizontal gradient would reflect abrupt lateral changes in magnetisation (Cordel and Grauch, 1987). The horizontal gradient is given by equation 4.

$$h(x,y) = \left[\left(\frac{\partial g_z(x,y)}{\partial x} \right)^2 + \left(\frac{\partial g_z(x,y)}{\partial y} \right)^2 \right]^{\frac{1}{2}} \quad \text{...(4)}$$

When applied to two-dimensional surveys, the horizontal gradient tends to place narrow ridges over abrupt changes in magnetisation. Location of maxima in horizontal gradient can be done by simple inspection. The assumption in this procedure is that the contrasts in physical properties such as magnetisation occur across vertical and abrupt boundaries isolated from other sources.

2.3   Reduction to the Pole

Positive gravity anomalies tend to be located over mass concentration but the same is not necessarily true for magnetic anomalies when the magnetisation and ambient field are not both directed vertically. In reduction to the pole procedure, the measured total field anomaly is transformed into the vertical component of the field caused by the same source distribution magnetised in the vertical direction. The acquired anomaly is therefore the one that would be measured at the north magnetic pole, where induced magnetisation and ambient field both are directed downwards (Blakely, 1995).

The software Euler was used in reducing to the pole the magnetic profile data. This was important for outlining magnetic units and positioning magnetic discontinuities, which may correspond to faults. Reduction to the pole is usually unreliable at low magnetic latitudes, where northerly striking magnetic features have little magnetic expression. Some bodies have no detectable magnetic anomaly at zero inclination (Blakely, 1995). The validity of the reduction to the pole is doubtful for inclinations lower than approximately 15º. The average inclination in the survey area was -25.27º and is located at average magnetic latitude of 10.47º and therefore reduction to the pole may be considered reliable.

3.0   Results and Discussion

From magnetic profile AA´ in Figure 4, calculated solutions map the depth to the subsurface structure. A structural index of 1.0 was used since it best represents sill edge, dike, or fault with limited throw. The horizontal and vertical gradients highly fluctuate over a distance of

14 km to 22 km along the profile. This may represent abrupt lateral change in magnetisation over the distance range. The depth to the magnetic structure is shallowest from 14-22 km at a depth of approximately 0.8 km from the surface. The deepest part of the profile was 8 km. The shoulder of the reduction to the pole (RTP) outlines the edges of a possible thick dyke located at profile distance 15-21 km.

From magnetic profile BB′ in Figure 5, solution cluster is observed at 11 km, 14 km, 17 km and 25 km. There is an abrupt change in both horizontal and vertical gradients between 14-16 km profile distances and also at the same location; the shallowest depth of approximately 0.5 km is attained along the profile. The shoulders of the RTP curve outlines the probable edges to causative structures at profile distances 7 km, 14 km, 17 km and 26 km. The main advantage of using this technique is that it provided a fast method for imaging approximate depths to subsurface bodies. The identified locations and depths to the causative sources are independent of magnetisation directions or distortion of field caused by remanent magnetism. The form of the feature was also inferred from the optimum structural index applied. The approximate source depth locations acquired were used later for start models in generating forward models.

From magnetic profile CC′ in Figure 6, a structural index of 1.0 was used and the solutions found reflected major discontinuities from 6 km, 9 km, 16 km and 21 km. These may represent faulted structures. There are also abrupt changes in both horizontal and vertical gradients at 17.5 km.
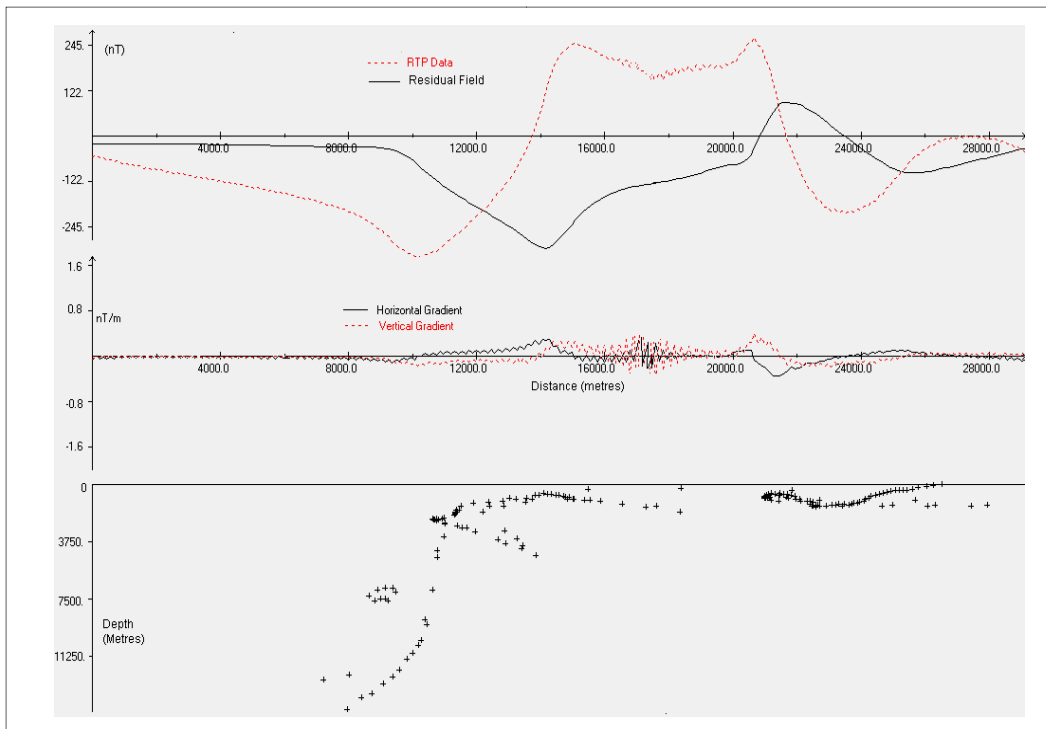

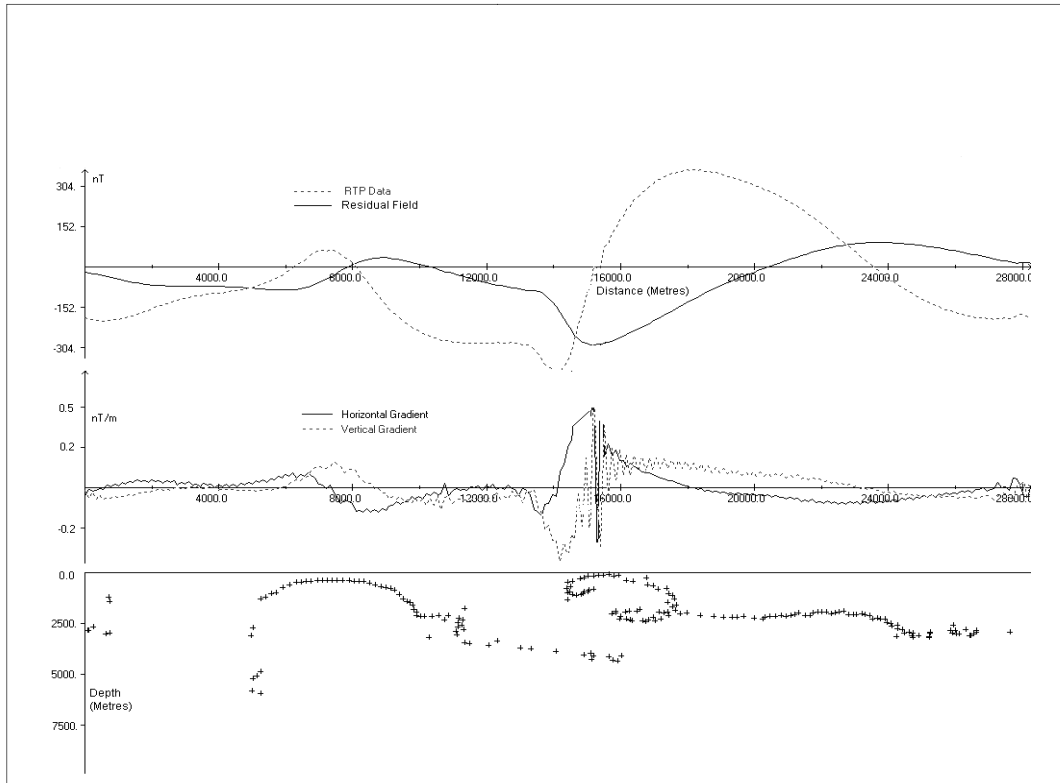*Figure 4: Euler depth solutions along magnetic anomaly profile AA′.*

Figure 5: Euler depth solutions along magnetic anomaly profile BB´.

The Euler solutions along the magnetic profile DD´ in Figure 7 maps the magnetic structure with the shallowest depth of 0.9 km and deepest at 4.2 km. The horizontal and vertical gradients fluctuate at a profile horizontal distance of 4 km and 12 km. This position also coincides with the inflection point of the corresponding RTP curve. This may represent the top of a magnetic body.
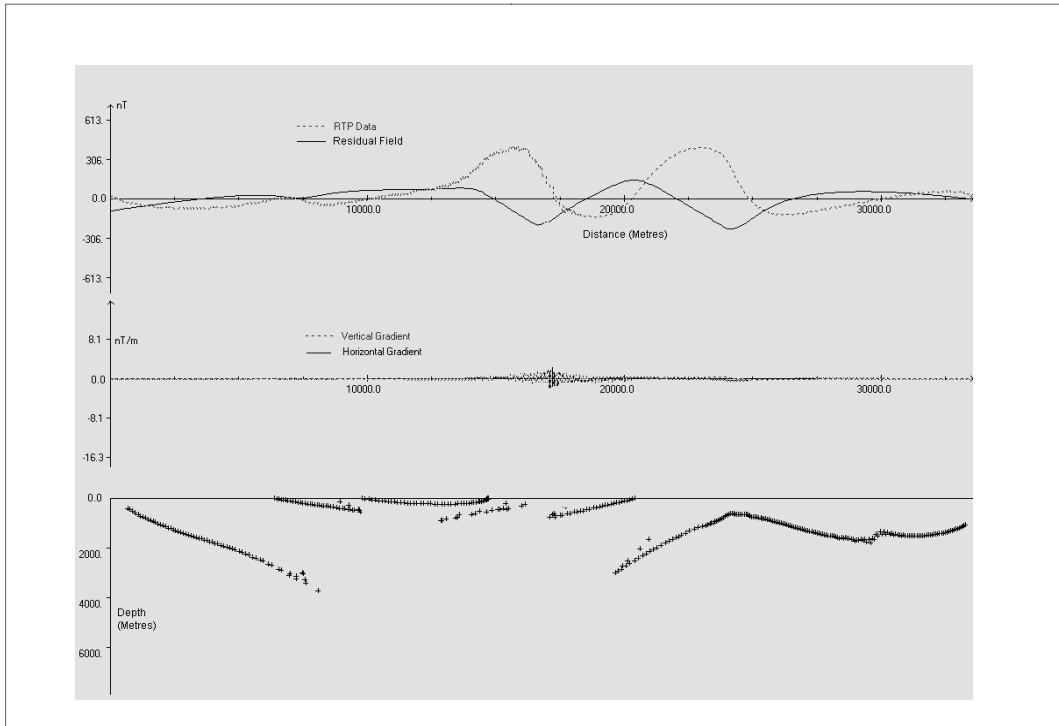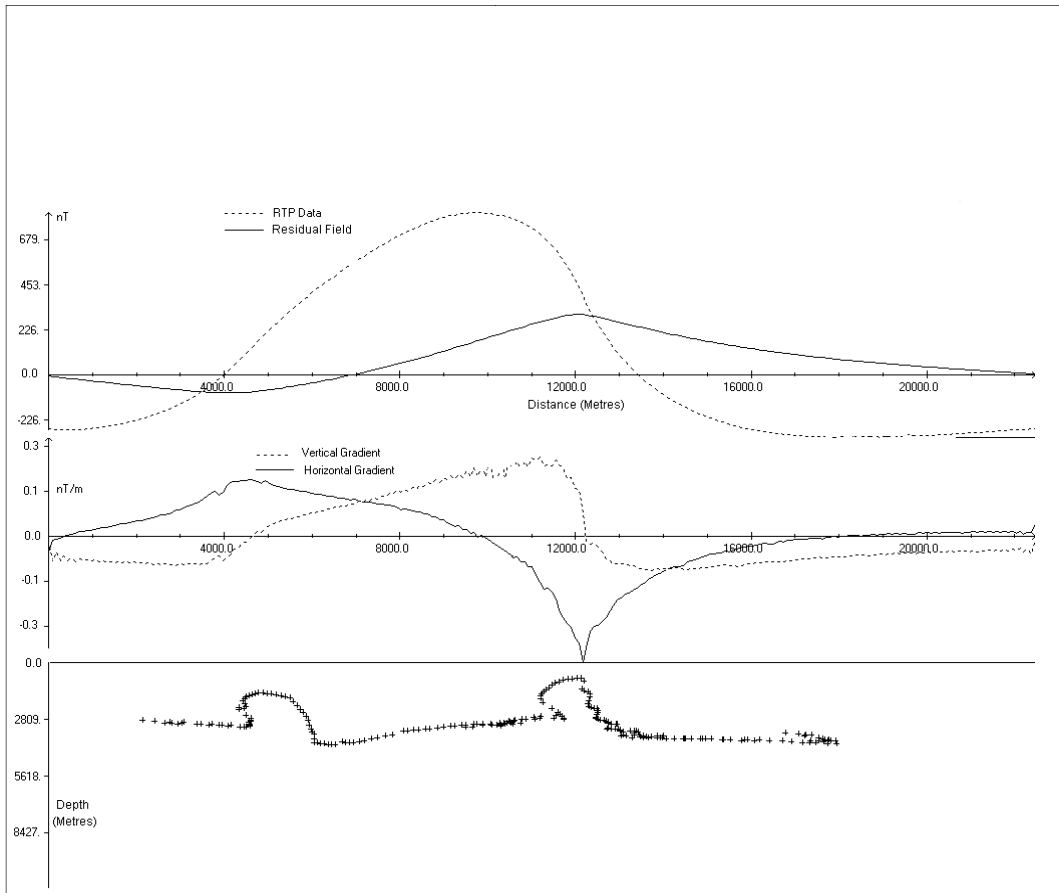
Figure 6: Euler depth solutions along magnetic anomaly profile CC′

Figure 7: Euler depth solutions along magnetic anomaly profile DD´

The Euler solutions along the magnetic profile EE´ in Figure 8 have the shallowest depth of 0.2 km and the deepest is 2 km. The RTP curve display a magnetic low at 7 km and a magnetic high at 13 km, which may represent rocks of low and high magnetic susceptibility respectively relative to the host rocks. Fluctuations of magnetic gradients are evident at 8 km, 13 km and 19 km possibly indicating changes in magnetisation. The Euler magnetic analysis along profile FF´ in Figure 9 reveals a shallow magnetic structure to a maximum depth of 1.7 km at a point of inflection of the magnetic anomaly curve. This is at a horizontal profile distance of 7 km. RTP curve has a maxima close to this point indicating the effect of the body at this point. There is a sudden change in the horizontal magnetic gradients at profile distances of 3 km, 4.5 km, 5.5 km and 9 km which may be points defining edges of the body where magnetisation changes.
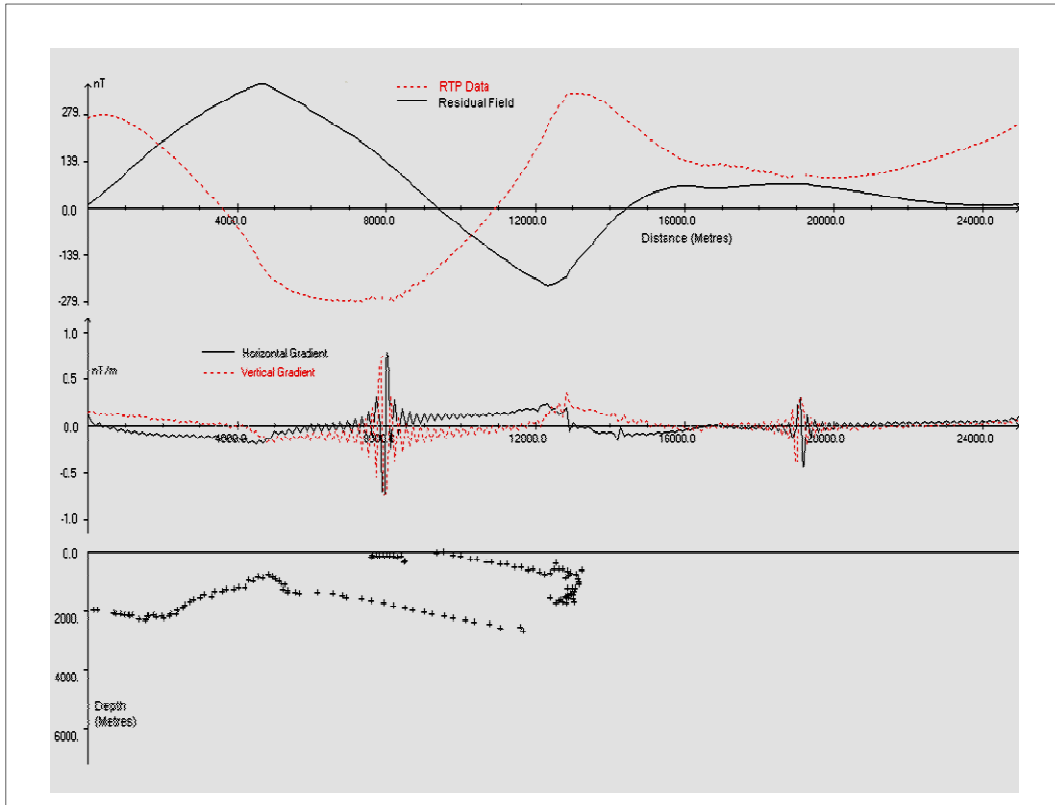
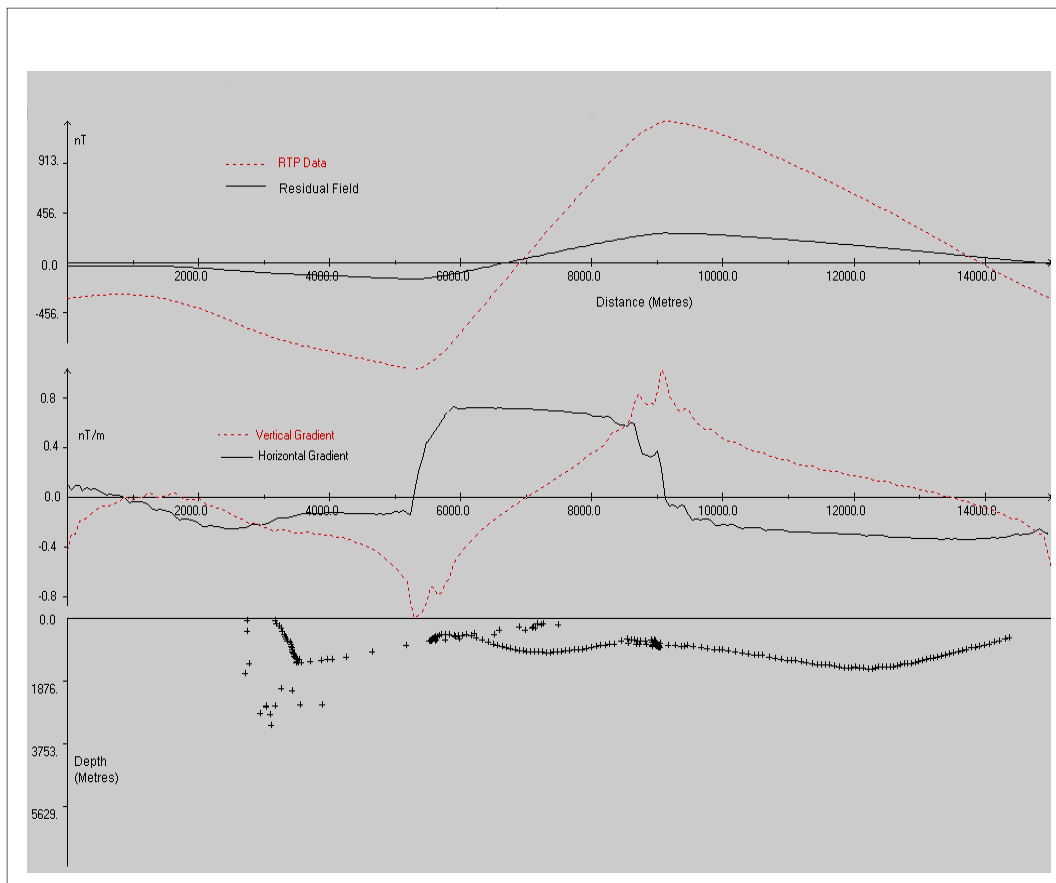Figure 8: Euler depth solutions along magnetic anomaly profile EE´

Figure 9: Euler depth solutions along magnetic anomaly profile FF´

Conclusion

The Euler deconvolution method has been effectively used in estimating depth to the top of magnetic bodies. Along the profiles AA´, BB´, CC´, DD´, EE´ and FF´, the depth to the bodies is variable ranging from the surface to about 11 km. This suggests presence of deep sedimentary basins in some regions in the study area. The profile anomaly AA´ in particular indicates sedimentary depth of about 11 km and the reduction to the pole cross-section is characteristic of a thick dyke. The dyke may be a possible heat source causing a thermal anomaly in the area surrounding Lake Magadi and such sedimentary basins may have been filled with sediments to the present time. Such a dyke is suspected to originate from a magma chamber conducting heat to the underground water. A model, whereby the faults in the region provide escape of water as hot springs, is proposed.

However, the use of Euler deconvolution in interpretation of potential fields for source depths and location developed by Reid *et al.,* (1990) is limited due to uncertainty of depth estimates generated and also absence of susceptibility, density contrast and dip estimates. Reid *et al.* (1990) suggest that for the structural index 1.0, the acceptance level to imaged depths is ±15%. The depths imaged in this study were therefore considered to an acceptance level of ±15% which may be used for an initial start model of the bodies for further detailed study.

References

Baker B.H. (1958). Geology of the Magadi area. *Report Geological survey of Kenya* 42. The Government printer, Nairobi.

Baker B.H. (1963). Geology of the area south of Magadi. *Report Geological survey of Kenya* 61. The Government printer, Nairobi.

Blakely R. J. (1995). Potential theory in Gravity and Magnetic applications. , pp. 70, 285-303 university press, Cambridge.

Cordell L., and Grauch, V.J.S. (1987). Mapping basement magnetisation zones from aeromagnetic data in the San Juan basin, New Mexico, in Hinze, W.J., Ed., The utility of regional gravity and magnetic anomaly maps: *Geophysics*, **52**, pp 181-197.

Gregory W. (1921). The rift valleys and geology of East Africa, pp. 479 Seeley Service London.

Hsu Shu-Kun (2002). Imaging magnetic sources using Euler's equation. *Geophysical prospecting*, **50**, pp 15-25.

Mushayandebvu, M.F., Van Driel, P., Reid, A.B. and Fairhead, J.D. (2001). Magnetic source parameters of two-dimensional structures using extended Euler deconvolution: *Geophysics*, **66**, pp 814-823.

Reid A.B., Allsop J.M., Granser H., Millets A.J., and Somerton I.W. (1990). Magnetic interpretation in three dimensions using Euler deconvolution. *Geophysics*, **55**, pp 80-91